


RESEARCH

Open Access



Fibrotic remodeling in joint diseases: induction and inhibition of fibrosis in fibroblast-like synoviocytes

Sofie Falkenløve Madsen^{1,2*} , Sarah Spliid Madsen^{1,2}, Alexander Scheller Madrid³, Mikkel Rathsach Andersen³, Anne-Christine Bay-Jensen² and Christian S. Thudium²

Abstract

Background We aimed to investigate the development of synovial fibrosis in vitro and how the fibrosis can be halted. Synovial fibrosis causes joint stiffness in arthritic diseases. The pathway of the fibrotic growth factor, transforming growth factor-beta (TGF- β), has been associated with joint pain in osteoarthritis (OA) and with the fibroid phenotype of rheumatoid arthritis (RA). This suggests that synovial fibrosis, thus accumulation of extracellular matrix (ECM) proteins, plays a role in the clinical manifestations of the diseases. Improving our understanding of fibrotic development may aid in selecting appropriate treatments and development of drugs that can target synovial fibrosis.

Methods We isolated primary fibroblast-like synoviocytes (FLS) from the synovial membrane of patients undergoing total knee replacement surgery. To investigate the development of synovial fibrosis, the FLS were cultured in a crowded in vitro model mimicking the ECM. TGF- β 1 was used as the fibrotic initiator, the activin receptor-like kinase 5 inhibitor (ALK5i), the anti-fibrotic drug nintedanib, and the anti-inflammatory drug tofacitinib were used as fibrotic inhibitors. The ECM protein formation was quantified in the conditioned media using specific biomarkers of type I, III, and VI collagen formation and fibronectin turnover.

Results The TGF- β stimulation induced fibrogenesis by increasing the biomarkers of fibronectin turnover, type I, III, and VI collagen formation. ALK5i and nintedanib inhibited the TGF- β response across all biomarkers. Tofacitinib trended towards inhibiting TGF- β response with up to 78% inhibition. All the treatments preserved cell viability.

Conclusion We have established an in vitro model for assessing fibrogenesis in primary FLS, which can be used to assess the anti-fibrotic effect of multiple drug types. Our study implies that synovial fibrosis can be induced by TGF- β , which additionally can be halted by both direct and indirect inhibition with anti-fibrotic substances. The anti-inflammatory drug tofacitinib also halted the fibrogenesis to some extent; thus, it may exert an anti-fibrotic effect.

Keywords Synovial fibrosis, Fibrogenesis, Osteoarthritis, Rheumatoid arthritis, Fibroblast-like synoviocytes, Synovial membrane, Scar-in-a-Jar, Anti-fibrotic drugs, Transforming growth factor-beta, Fibrosis

*Correspondence:

Sofie Falkenløve Madsen
som@nordicbio.com

¹Department of Biomedical Sciences, University of Copenhagen, Blegdamsvej 3, København N, Copenhagen 2200, Denmark

²ImmunoScience, Nordic Bioscience, Herlev Hovedgade 205, Herlev 2730, Denmark

³Orthopedic Surgery Unit, Gentofte Hospital, Gentofte Hospitalsvej 1, Hellerup 2900, Denmark



© The Author(s) 2024. **Open Access** This article is licensed under a Creative Commons Attribution 4.0 International License, which permits use, sharing, adaptation, distribution and reproduction in any medium or format, as long as you give appropriate credit to the original author(s) and the source, provide a link to the Creative Commons licence, and indicate if changes were made. The images or other third party material in this article are included in the article's Creative Commons licence, unless indicated otherwise in a credit line to the material. If material is not included in the article's Creative Commons licence and your intended use is not permitted by statutory regulation or exceeds the permitted use, you will need to obtain permission directly from the copyright holder. To view a copy of this licence, visit <http://creativecommons.org/licenses/by/4.0/>.

Background

Patients diagnosed with rheumatoid arthritis (RA) and osteoarthritis (OA) frequently experience joint stiffness and pain [1, 2]. The joint stiffness is caused by synovial fibrosis, which occurs after excessive extracellular matrix (ECM) protein deposition [3]. The cause of fibrogenesis in joints has not yet been elucidated. While high levels of the known fibrotic growth factor transforming growth factor beta (TGF- β) and accumulations of collagens have been found in patients with RA and OA [3–7]. The current treatment for rheumatic patients is anti-inflammatory, while up to 50% of patients with RA do not respond to the first line of treatment [8, 9]. The inadequate response can potentially be caused by synovial fibrosis. Previous findings in the literature have focused on the presence of fibrosis or related proteins and not the fibrotic process in the joints [6, 7, 10–15]. Thus, there is a lack of models to investigate fibrogenesis in the joints, how it is triggered, and how it can be inhibited. A broader understanding of the fibrotic process may aid in determining if an anti-fibrotic focus can increase the response rate in patients.

The TGF- β pathway has been indicated in disease development in both RA and OA [3, 14–16]. In early-stage OA, pain has been associated with the upregulation of TGF- β and Suppressor of Mothers Against Decapentaplegic (SMAD) [16]. Moreover, patients with RA presenting the fibroid phenotype have upregulated signaling of TGF- β , SMAD, and bone morphogenic protein (BMP) compared to the inflammatory phenotypes [15]. TGF- β is found in high levels in the synovial membrane and fluid in both OA and RA [3–5, 14–16]. Thus, TGF- β is present in the synovial joints and is related to both pain and fibrosis.

TGF- β activates fibroblasts and fibroblast-like synoviocytes (FLS) to myofibroblasts. Myofibroblasts have a higher formation of ECM proteins, such as collagens and fibronectin [3–5]. In arthritis diseases, the ECM composition of the joint changes [6, 7, 10]. In a healthy synovium, type I collagen is present in the lining of the synovium, and the ECM is composed of fibronectin, type III, and VI collagen, among other proteins [10–12]. The OA synovium is thickened with a collagenous matrix and small areas of fibronectin compared to healthy. The RA synovium is inflamed with high fibronectin and small areas of fibrosis compared to healthy [6, 7, 12]. In addition to histology, chromatography investigations show increased type III collagen in RA biopsies [13]. In the fibroid phenotype of RA, gene expression studies on biopsies show upregulation of multiple collagens, including type I and III collagen, compared to the inflammatory phenotypes [14, 15]. The ECM composition investigations are based on patient biopsies [6, 7, 10–15]. From

a biopsy, information about the fibrotic state and ECM composition at that specific time can be investigated.

Preclinical models are often used to investigate the process of synovial fibrosis. Biopsies in a collagen-induced OA mice model were also used to investigate fibrosis, as in patients. However, in vivo, the animals were sacrificed to obtain the biopsies. Hence, the in vivo model cannot investigate synovial fibrosis over time within the same animal. However, TGF- β stimulation in vivo leads to persistent fibrosis assessed by histology and upregulated gene expression of type I collagen and several enzymes related to fibrosis [17]. When primary FLS is cultured and stimulated with TGF- β , the gene expression of multiple enzymes, fibronectin, type I and II collagen are upregulated [18]. The histology and upregulated genes found preclinically correlate to what is found in patients [6, 7, 12, 14, 15]. However, gene expression does not directly reflect protein levels or fibrogenesis [19]. Thus, to investigate the development of synovial fibrosis and fibrogenesis, the protein levels need to be included in the assessments.

Depending on the preclinical model, different parts of the synovial fibrosis can be assessed. Ex vivo models contain degradation products from fibrolysis but lack fibrogenesis [20]. The lack of fibrogenesis in ex vivo models might be caused by the fibroblasts leaving the tissue during culturing, which is also a common way to isolate the fibroblasts [17]. Standard monolayer in vitro models only produce non-functional procollagens and no degradation enzymes; thus, they reflect neither fibrolysis nor fibrogenesis [20–24]. However, adding macromolecular crowders in vitro can change this, leading to a pseudo-3D environment [21–24]. The crowded environment leads to rapid production of mature and functional collagen molecules within days, indicating fibrogenesis in vitro [21, 25]. The collagens can be assessed with Sirius red staining; however, this cannot determine the specific collagens [22, 26, 27]. Fibrogenesis-specific proteins can be assessed with biomarkers in the supernatant [27–29]. Using joint FLS in a crowded environment could potentially lead to an in vitro model, which enables us to investigate the protein levels in fibrogenesis.

A fibrogenesis model could increase our understanding of synovial fibrosis development and how to potentially inhibit it. In preclinical models, TGF- β stimulation is often used to initiate fibrosis [3, 14–16]. Moreover, inhibition of TGF- β indicates inhibition of fibrosis. In OA-FLS, this has been shown with type I collagen gene expression: TGF- β stimulation induces the gene expression and is halted by inhibition of activin receptor-like kinase (ALK; TGF- β type I receptor, TGF β RI) [30]. TGF- β stimulation induces protein levels of fibronectin and type I, III, and VI collagen in vitro with crowding using healthy skin and pulmonary fibroblasts. The induced protein levels in

healthy fibroblasts are inhibited by both an ALK5 inhibitor and nintedanib [28, 29]. Nintedanib, a tyrosine kinase inhibitor, indirectly inhibits TGF- β signaling by preventing activation of TGF β RII [31].

Currently, it is difficult to investigate the changes and accumulation of ECM protein levels relating to synovial fibrosis both clinically and preclinically. The present preclinical models can investigate gene expression but do not directly reflect protein levels or fibrogenesis [19]. To broaden our understanding of fibrogenesis in the joints, we investigated the formation of ECM proteins from primary FLS from joints in an in vitro model with macromolecular crowders. The formation of ECM proteins was investigated with biomarkers that can be used both preclinically and in patients, which enables the preclinical results to be translational to potential clinical results. TGF- β 1 stimulation was used to initiate a fibrotic response. Furthermore, we investigated the inhibitory effect of ALK5i, nintedanib, and the Janus kinase (JAK) inhibitor tofacitinib on the fibrotic response. ALK5i directly inhibits TGF- β 1 stimulation, while nintedanib indirectly inhibits it [31, 32]. Tofacitinib targets the JAK receptors but has been shown to inhibit type I collagen gene expression promoted by TGF- β 1 in combination with interleukin-6 in FLS [33]. A broader understanding of fibrogenesis in the joints may aid in selecting appropriate treatments and developing drugs that can target synovial fibrosis.

Materials and methods

Human synovial tissue

FLS was isolated from synovial tissue collected from patients undergoing total knee replacement surgery at Gentofte Hospital, Denmark. The study was conducted in accordance with the Declaration of Helsinki, and all patients gave written informed consent prior to surgery. The collection was approved by the Danish Scientific Ethical Commission (protocol no. H-D-2007-0084). The collection did not involve additional risk for the patients, as the synovial tissue was removed in relation to the surgery. The patient information recorded was sex, age, and disease (OA or RA) (Additional file 1; Table S1). For this study, we collected FLS from 13 patients undergoing surgery because of severe OA.

Isolation of joint fibroblast-like synoviocytes

The synovial tissue was collected and stored in Dulbecco's modified eagle medium (DMEM)+GlutaMax (Gibco, Life Technologies, Carlsbad, California, USA cat. no. 31,966) with 1% Penicillin/Streptomycin (P/S) (Sigma-Aldrich, cat. no. P4333) at 4 °C. The visible fat on the synovial tissue was removed with a scalpel, followed by a rinse in Dulbecco's phosphate-buffered saline (PBS) (Sigma-Aldrich, cat. no. D8537) to remove excess

fat. The synovial tissue was weighed and minced. The tissue was digested in digestion media (20 mL/g tissue) at 300 rpm for 2 h at 37 °C to separate the FLS from the tissue. The digestion media was 10% fetal bovine serum (FBS) (Sigma-Aldrich, St. Louis, Missouri, USA, cat. no. F7524) Roswell Park Memorial Institute (RPMI)-1640 medium without L-glutamine (Sigma-Aldrich, cat. no. R0883) with 1% P/S, with 1 mg/mL Collagenase Type II (Worthington, Lakewood, New Jersey, USA, cat. no. 40A1995I). The digestion media was filtered through a 70 μ m cell strainer followed by a 0.2 μ m filter before use. The digested synovial tissue was filtrated through a 70 μ m cell strainer and centrifuged at 220 g for 5 min. The pellet was resuspended in 10% FBS RPMI, transferred to a T25 flask, and cultured at 37 °C, 5% CO₂ [20]. The media was changed two to three times a week, and the cells were split when they reached 80% confluency. The FLS were frozen down at passages 2–4.

Fibroblast cell culture: Scar-in-a-Jar

The primary FLS were cultured at passage 3–5 in 10% FBS RPMI. The FLS were seeded at 100,000 cells/mL in 48-well plates in 10% FBS DMEM and incubated overnight at 37 °C, 5% CO₂. The cells were serum-starved in 0.4% FBS DMEM and incubated overnight at 37 °C, 5% CO₂, to avoid serum interference with biomarkers measurements. To obtain the crowded environment used in the Scar-in-a-Jar (SiaJ) model, 0.4% FBS DMEM media was mixed with ficoll 70 (56.25 mg/mL; GE Healthcare, Chicago, Illinois, USA, cat. no. 17,031,050), ficoll 400 (37.5 mg/mL; GE Healthcare, cat. no. 17,030,050) and L-ascorbic acid 2-phosphate (50 μ g/mL; Wako, Osaka, Japan cat. no. 013-19641) [22]. At the beginning of the experiment, day 0, 200 μ L of the 0.4% FBS ficoll DMEM media was added, together with 100 μ L of appropriate treatment to each well. Each study contained a control of non-stimulated FLS (without, w/o), where 100 μ L of 0.4% FBS DMEM was added instead of treatment media. The supernatant was collected on days 0, 4, 8, and 12 of the experiment. Fresh treatment was added on days 4 and 8. TGF- β 1 [24–800 pM] (R&D Systems, Minneapolis, Minnesota, USA, cat. no. 240-B) was used as the fibrotic growth factor. The response of TGF- β 1 was inhibited with ALK5i [10–1000 nM] (SB-525,334; Sigma-Aldrich, cat. no. S8822), nintedanib [10–1000 nM] (Kemprotec Ltd., Smalithorn, Carnforth, UK) and tofacitinib [12.5–100 μ M] (citrate, CAS no. 540737-29-9; Sigma-Aldrich, cat. no. PZ0017). The induction and inhibitory concentrations used in the experiments are based on previous experiences in the SiaJ model and the literature [28, 29, 31, 34–36]. The inhibitors were added alone or together with TGF- β 1. Each experiment had two to four technical replicates of each treatment in each FLS donor.

The supernatant was stored at $-20\text{ }^{\circ}\text{C}$ until biomarker measurements.

Cell viability

Metabolic activity was assessed at the beginning (day 0) and the end (day 12) of the cell culture experiment. The alamarBlue (Invitrogen, Carlsbad, California, USA cat. no. DAL1015) assay was used and carried out according to the manufacturer's guidelines. The FLS were incubated in 10% alamarBlue in 0.4% FBS DMEM for two hours at $37\text{ }^{\circ}\text{C}$, 5% CO_2 . The conditioned media was transferred to black plates (Corning, New York, USA, cat. no. 3915) and read at 540 nm/590 nm (excitation/emission wavelengths) in a fluorescence microplate reader (SpectraMax, Molecular Devices, San Jose, California, USA). The cell viability is based on the metabolic activity of living cells, which reduces resazurin to resorufin. If no fluorescence was detected, the cells were presumed dead.

Enzyme-linked immunosorbent assays

ECM formation and turnover biomarkers were measured in the collected supernatant. The biomarkers were technically validated competitive enzyme-linked immunosorbent assays (ELISAs) of type I, III, and VI collagen formation and fibronectin turnover (PRO-C1 cat. no. 2800, PRO-C3 cat. no. 1700, PRO-C6 cat. no. 4000, and FBN-C, cat. no. 0101, respectively; Nordic Bioscience, Herlev, Denmark) [37–40]. The assays were performed according to the manufacturer's instructions. Briefly, a streptavidin-coated plate was incubated with a biotinylated antigen solution for 30 mins at $20\text{ }^{\circ}\text{C}$. Standards, quality controls, and samples were added with the subsequent addition of peroxidase-conjugated monoclonal antibodies. This was then incubated for either 3 hours (PRO-C1) or 20 hours (PRO-C3, PRO-C6, and FBN-C) at $4\text{ }^{\circ}\text{C}$. After a wash, the plates were incubated with the substrate (3,3',5,5'-tetramethylbenzidine (TMB ONE), Kementec, Taastrup, Denmark, cat. no. 4380) for 15 min at $20\text{ }^{\circ}\text{C}$. The reaction was stopped with 0.18 M sulfuric acid (Sigma-Aldrich, cat. no. 30,743). The absorbance was measured using 450 nm with 650 nm as a reference on an absorbance microplate reader (Multiskan Sky, ThermoFisher) [37–40]. Concentrations were calculated based on a four-parametric standard curve. Samples above the measurement range were diluted and reanalyzed. Samples below the measurement range were given the lowest measured concentration for statistical purposes. For PRO-C3 measurements, 0.1 ng/mL was used, and for PRO-C6, 0.07 ng/mL. No samples were below the measurement range in PRO-C1 and FBN-C.

Statistics

The viability was assessed using the raw data, as the data was already normally distributed. The treatments were

compared with one-way repeated measures analysis of variance (ANOVA) with Tukey's or Dunnett's multiple comparisons tests. The viability is displayed as the fluorescence values, with box plots with whiskers and dots indicating the value of each donor.

The biomarker measurements were log-transformed to obtain a normal distribution. The log-transformed data were compared with two-way ANOVA with Tukey's or Dunnett's multiple comparisons tests. The values are displayed as the geometric mean \pm 95% confidence interval (CI). The raw biomarker values' area under the curve (AUC) was computed for a comprehensive overview. The AUC was compared with repeated measures one-way repeated measures ANOVA with Tukey's or Dunnett's multiple comparisons tests. Graphical illustrations and statistical tests were performed using GraphPad Prism version 9.5 (GraphPad Software). P -values ≤ 0.05 were considered statistically significant; asterisks (or other symbols specified) indicate * $p < 0.05$, ** $p < 0.01$, *** $p < 0.001$, and **** $p < 0.0001$.

Results

Induction of fibrotic response

The primary FLS were stimulated with TGF- β to assess the capacity for ECM protein formation. Based on previous investigations in healthy dermal and pulmonary fibroblasts in the SiaJ model, we chose to test three doses of TGF- β (24, 80, and 800 pM) to identify the maximum response [27]. Cell viability measurements and biomarkers of ECM formation and turnover assessed the response.

The fibrotic response was initially tested with TGF- β [24 pM] and [80 pM] in three donors (Additional file 1; Figure S1, S2). The viability of the FLS was assessed as a surrogate for metabolic active and alive fibroblasts. The assessment was used to evaluate the viability of all individual wells and patients, confirming the unity assumption. TGF- β [24 pM] and [80 pM] both increased the viability compared to w/o ($p < 0.001$) (Additional file 1; Figure S1). The ECM protein biomarkers were increased to different extents within the three FLS donors (Additional file 1; Figure S2). Thus, more donors were investigated with TGF- β [80 pM] and [800 pM].

Eight donors were used to investigate the fibrotic response of TGF- β [80 pM] and [800 pM]. Both TGF- β [80 pM] and [800 pM] increased the viability compared to the control ($p < 0.001$, Fig. 1). TGF- β [800 pM] also increased the viability compared to TGF- β [80 pM] ($p < 0.05$, Fig. 1).

TGF- β [80 pM] and [800 pM] both increased PRO-C1 from day 4 and onwards compared to the control and were not different from each other on any of the days ($p < 0.0001$, Fig. 2A). Both doses of TGF- β increased the PRO-C1 AUC, while TGF- β [800 pM] achieved a

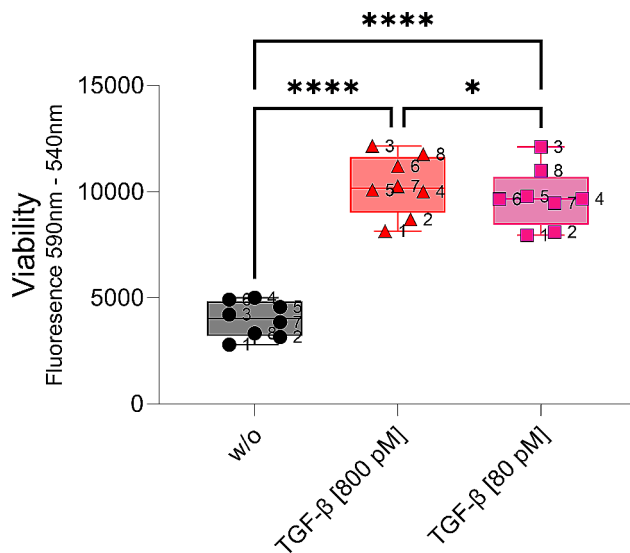


Fig. 1 The viability after 12 days of TGF- β stimulation. The data are shown as a box plot with lines indicating the 25-, 50-, and 75-percentiles, with the whiskers indicating minimum to maximum. The symbols and numbers indicate the different donors. The experiment was conducted on 8 donors, namely donors 1–8. The data was compared with a one-way repeated measures ANOVA with Tukey's multiple comparisons test. P -values ≤ 0.05 were considered statistically significant. Asterisks indicate: * $p < 0.05$, ** $p < 0.01$, *** $p < 0.001$, and **** $p < 0.0001$

higher AUC than TGF- β [80 pM] ($p < 0.0001$, $p < 0.001$ and $p < 0.05$, respectively; Fig. 2B). Both TGF- β doses increased PRO-C3 from day 8 compared to the control and did not differ from each other ($p < 0.0001$, Fig. 2C). The PRO-C3 AUC was also increased by both doses ($p < 0.01$ and $p < 0.05$, Figure 2D). TGF- β increased PRO-C6 on days 4, 8, and 12 compared to the control ($p < 0.05$, $p < 0.001$, and $p < 0.0001$, respectively, Figure 2E). Both doses of TGF- β similarly increased the AUC compared to the control ($p < 0.0001$, Fig. 2F). FBN-C was increased from day 4 and onwards by both TGF- β doses ($p < 0.0001$, Fig. 2G). The AUC of FBN-C was increased by both TGF- β doses ($p < 0.001$, Fig. 2H). The response to the TGF- β [80 pM] and [800 pM] doses was only different in the PRO-C1 AUC assessment (Fig. 2A). Due to the limited difference, TGF- β [80 pM] was chosen for further studies.

Inhibition with ALK5i

The fibrotic response to TGF- β [80 pM] was inhibited using ALK5i, a TGF- β type I receptor inhibitor. Non-stimulated fibroblasts (w/o) and ALK5i [1000 nM] were negative controls. Three doses of ALK5i (10, 100, and 1000 nM) were added together with TGF- β [80 pM] to assess inhibition. Five FLS donors were used for this assessment.

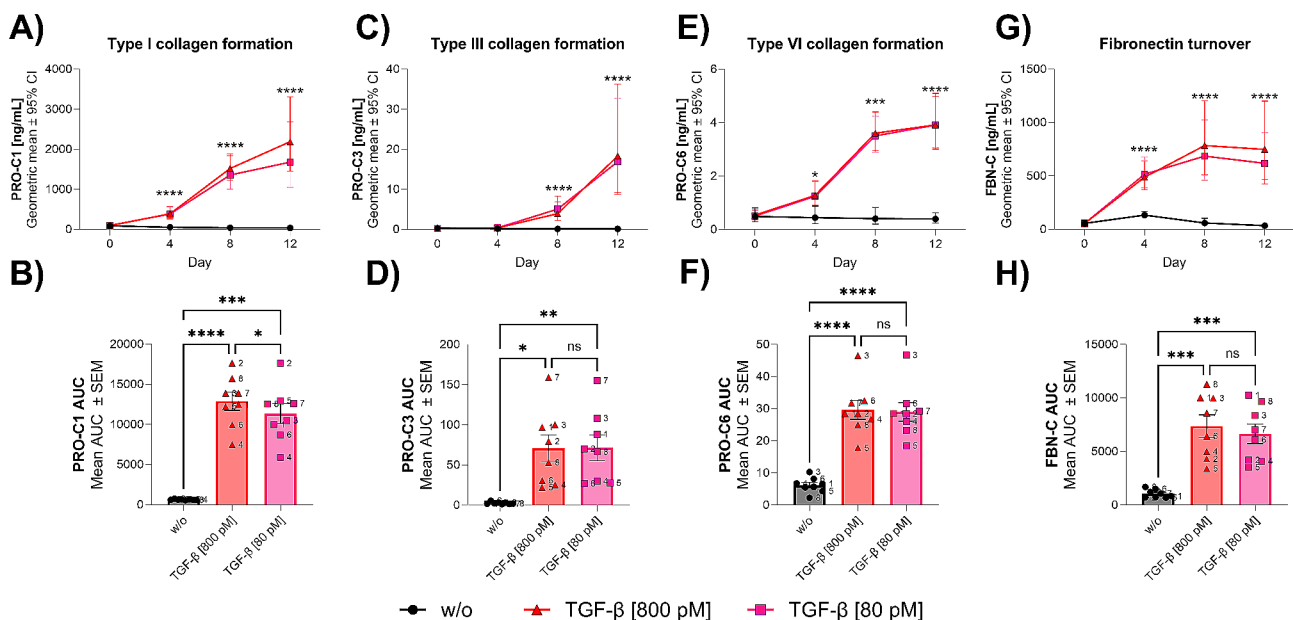


Fig. 2 The biomarker response of FLS to TGF- β stimulation. The data are shown as the geometric mean \pm 95% CI of each biomarker over the 12 days: type I (A), type III (C), type VI (E) collagen formation, and fibronectin turnover (G). The AUC is shown as mean AUC \pm SEM: type I (B), type III (D), type VI (F) collagen formation, and fibronectin turnover (H). The experiment was carried out with eight donors: donors 1–8. The symbols and numbers indicate the different donors. The biomarker values were log-transformed to obtain a normal distribution and were compared with two-way ANOVA with Tukey's multiple comparisons test on different days. The AUC was computed based on the raw biomarker values and compared with one-way repeated measures ANOVA with Tukey's multiple comparisons tests. P -values ≤ 0.05 were considered statistically significant. Asterisks indicate: * $p < 0.05$, ** $p < 0.01$, *** $p < 0.001$, and **** $p < 0.0001$. ns indicates no significant differences

The viability of TGF- β stimulated FLS was increased compared to the control (w/o) and ALK5i [1000 nM] ($p < 0.001$, Additional file 1; Figure S3). TGF- β +ALK5i [1000 nM] and TGF- β +ALK5i [100 nM] reduced the viability compared to TGF- β alone ($p < 0.001$, and $p < 0.01$; Additional file 1; Figure S3). TGF- β +ALK5i [10 nM] did not affect the viability. Viability was maintained within all treatment groups. Thus, the inhibitor was not toxic to the cells.

The control (w/o) was lower than single stimulation of TGF- β from day 4 in PRO-C1 and FBN-C, and from day 8 in PRO-C3 and PRO-C6, and within the AUC of all biomarkers ($p < 0.05$, Fig. 3). The ALK5i [1000 nM] control was lower than TGF- β from day 4 in PRO-C1, PRO-C6, and FBN-C and day 8 in PRO-C3 ($p < 0.05$, Fig. 3A, C, E, G). The AUC of the ALK5i [1000 nM] control was also lower than TGF- β within all assessed biomarkers ($p < 0.05$, Fig. 3B, D, F, H).

The PRO-C1 response of TGF- β was reduced by ALK5i [1000 nM] from day 4 ($p < 0.01$, $p < 0.0001$, and $p < 0.001$, respectively), while ALK5i [100 nM] reduced the PRO-C1 response from day 8 ($p < 0.05$; Fig. 3A). Similarly, the TGF- β induced PRO-C1 AUC was inhibited by both ALK5i [1000 nM] and [100 nM] ($p < 0.05$; Fig. 3B). The PRO-C3 response of TGF- β was reduced by ALK5i [1000 nM] from day 8 ($p < 0.01$ and $p < 0.001$, respectively),

while ALK5i [100 nM] reduced the response on day 12 ($p < 0.05$; Fig. 3C). The TGF- β induced PRO-C3 AUC response was similarly inhibited by both ALK5i [1000 nM] and [100 nM] ($p < 0.05$; Fig. 3D). Only ALK5i [1000 nM] was able to reduce the TGF- β induced PRO-C6 response and reduced it from day 8 ($p < 0.01$; Fig. 3E). Both ALK5i [1000 nM] and [100 nM] inhibited the TGF- β induced PRO-C6 AUC ($p < 0.05$; Fig. 3F). The TGF- β induced FBN-C was reduced from day 4 by ALK5i [1000 nM] ($p < 0.01$, $p < 0.001$, and $p < 0.001$, respectively), while ALK5i [100 nM] reduced the response on day 12 ($p < 0.001$; Fig. 3G). The TGF- β induced FBN-C AUC response was only inhibited by ALK5i [1000 nM] ($p < 0.05$; Fig. 3H). ALK5i [10 nM] was not able to inhibit the TGF- β response in any of the biomarkers (Fig. 3).

Inhibition with Nintedanib

The anti-fibrotic drug nintedanib was used to characterize the effect of indirect inhibition of TGF- β [80 pM] and the related fibrotic response. Non-stimulated fibroblasts (w/o) and Nintedanib [1000 nM] was used as negative controls. Three doses of nintedanib (10, 100, and 1000 nM) were added together with TGF- β [80 pM] to assess inhibition on seven FLS donors.

TGF- β increased the viability compared to the control (w/o) and Nintedanib [1000 nM] after 12 days

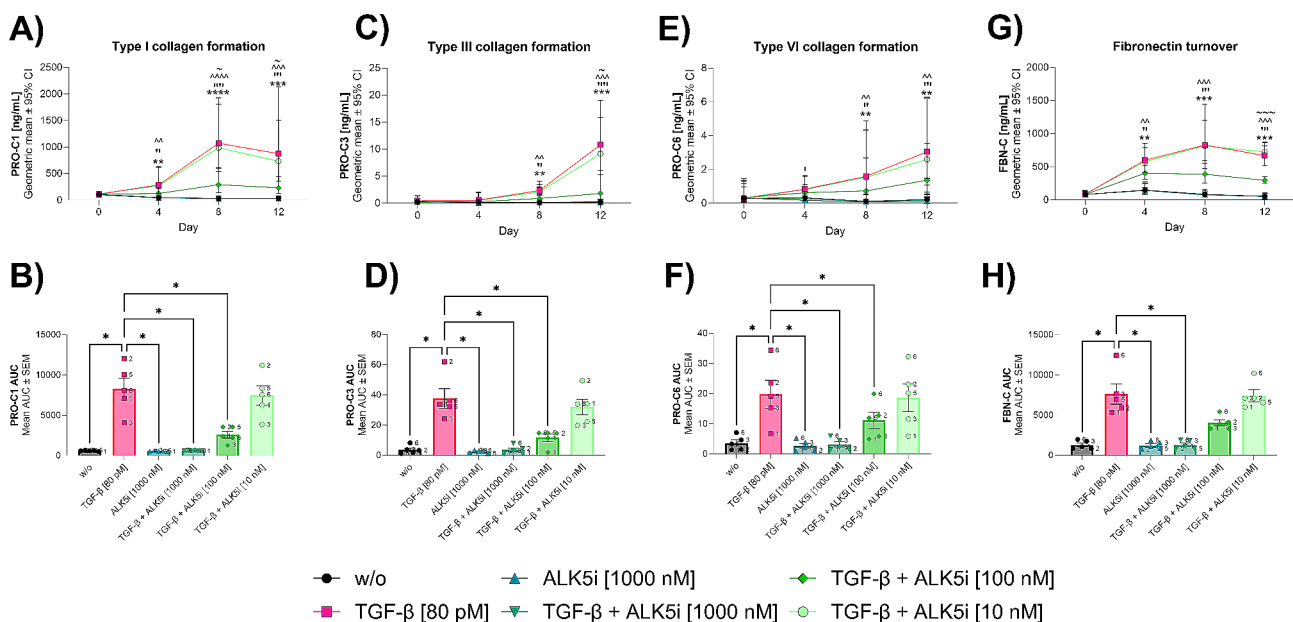


Fig. 3 The inhibition effect of ALK5i on TGF- β induction. The data are shown as the geometric mean \pm 95% CI of each biomarker over the 12 days: type I (A), type III (C), type VI (E) collagen formation, and fibronectin turnover (G). The AUC is shown as mean AUC \pm SEM: type I (B), type III (D), type VI (F) collagen formation, and fibronectin turnover (H). Five different FLS donors were used in this assessment: donors 1, 2, 3, 5, and 6. The symbols and numbers indicate the different donors. The biomarker values were log-transformed to obtain a normal distribution and were compared with two-way ANOVA with Dunnett's multiple comparisons test on different days. The AUC was computed based on the raw biomarker values and then compared with one-way repeated measures ANOVA with Dunnett's multiple comparisons tests. P -values ≤ 0.05 were considered statistically significant. Asterisks indicate: * $p < 0.05$, ** $p < 0.01$, *** $p < 0.001$, and **** $p < 0.0001$. In the time overview, different symbols indicate the comparisons to TGF- β : * w/o, ^ ALK5i, ^ TGF- β +ALK5i [1000 nM] and ~TGF- β +ALK5i [100 nM]

of treatment ($p < 0.001$, Additional file 1; Figure S4). TGF- β +Nintedanib [1000 nM] and TGF- β +Nintedanib [100 nM] reduced the viability compared to TGF- β ($p < 0.001$ and $p < 0.01$; Additional file 1; Figure S4). TGF- β +Nintedanib [10 nM] did not affect the viability. Viability was maintained within all treatment groups. Thus, nintedanib was not toxic for the cells.

The control (w/o) and Nintedanib [1000 nM] were lower than TGF- β from day 4 in PRO-C1, PRO-C3, and FBN-C, and from day 8 in PRO-C6, and within the AUC of all the biomarkers ($p < 0.05$, Fig. 4).

TGF- β +Nintedanib [1000 nM] reduced the PRO-C1 response from day 4 compared to TGF- β ($p < 0.01$), and the PRO-C1 AUC ($p < 0.001$, Fig. 4A-B). TGF- β +Nintedanib [100 nM] did not affect the TGF- β PRO-C1 response on any day, while the PRO-C1 AUC was reduced compared to TGF- β alone ($p < 0.05$, Fig. 4A-B). TGF- β +Nintedanib [1000 nM] reduced the PRO-C3 response of TGF- β on days 8 and 12, while TGF- β +Nintedanib [100 nM] reduced the response on day 12 compared to TGF- β ($p < 0.01$, $p < 0.01$, and $p < 0.05$, respectively, Figure 4C). Both TGF- β +Nintedanib [1000 nM] and [100 nM] reduced the TGF- β induced PRO-C3 AUC response compared to the TGF- β response ($p < 0.01$, Fig. 4D). TGF- β +Nintedanib [1000 nM] reduced the PRO-C6 response on days 8 and 12 compared to TGF- β ($p < 0.05$ and $p < 0.001$, Figure 4E). The PRO-C6 AUC

response was reduced by TGF- β +Nintedanib [1000 nM] and [10 nM] compared to TGF- β ($p < 0.05$, Fig. 4F). TGF- β +Nintedanib [1000 nM] reduced the FBN-C response from day 4 and onwards compared to TGF- β ($p < 0.001$, $p < 0.0001$, and $p < 0.0001$, respectively, Figure 4G). Nintedanib [1000 nM] also reduced the FBN-C AUC response compared to TGF- β alone ($p < 0.001$, Fig. 4H).

Inhibition with Tofacitinib

Tofacitinib has been shown to have an inhibitory effect on both skin and pulmonary fibrosis ex vivo; thus, we also characterized the anti-fibrotic effect of Tofacitinib in this system [41]. TGF- β [80 pM] was used to induce fibrogenesis, and non-stimulated fibroblasts (w/o) and Tofacitinib [100 μ M] was used as negative controls. Four doses of Tofacitinib (12.5, 25, 50, and 100 μ M) were added together with TGF- β [80 pM] to assess inhibition on three FLS donors.

The viability of TGF- β was higher than both the control (w/o) and single stimulation of Tofacitinib [100 μ M] ($p < 0.05$, Additional file 1; Figure S5). TGF- β +Tofacitinib [100 μ M] reduced the viability compared to TGF- β alone ($p < 0.01$, Additional file 1; Figure S5). TGF- β +Tofacitinib [12.5, 25, and 50 μ M] did not change the viability compared to TGF- β , and the viability was maintained within all treatment groups (Additional file 1; Figure S5).

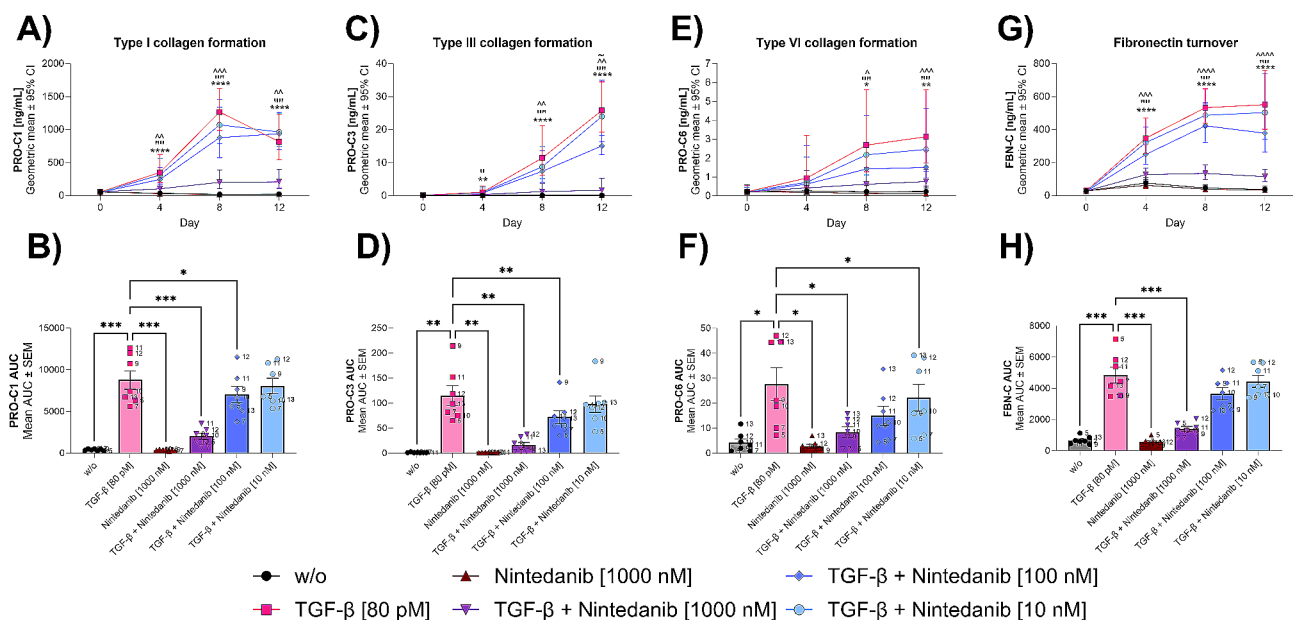


Fig. 4 The inhibitory effect of Nintedanib on TGF- β induction. The data are shown as the geometric mean \pm 95% CI of each biomarker over the 12 days: type I (A), type III (C), type VI (E) collagen formation, and fibronectin turnover (G). The AUC is shown as mean AUC \pm SEM: type I (B), type III (D), type VI (F) collagen formation, and fibronectin turnover (H). Each symbol represents a patient, and seven FLS donors were used, namely donors 5, 7, 9, 10, 11, 12, and 13. The symbols and numbers indicate the different donors. The biomarker values were log-transformed to obtain a normal distribution and were compared with two-way ANOVA with Dunnett's multiple comparisons test on different days. The AUC was computed based on the raw biomarker values and then compared with one-way repeated measures ANOVA with Dunnett's multiple comparisons tests. P -values ≤ 0.05 were considered statistically significant. Asterisks indicate: * $p < 0.05$, ** $p < 0.01$, *** $p < 0.001$, and **** $p < 0.0001$. In the time overview, different symbols indicate the comparisons to TGF- β : * w/o, ^ Nintedanib [1000 nM], ^ TGF- β +Nintedanib [1000 nM], and ~ TGF- β +Nintedanib [100 nM]

The response of the control (w/o) and Tofacitinib [100 μ m] were lower than TGF- β from day 4 in PRO-C1 and FBN-C, from day 8 in PRO-C3 and on day 8 in PRO-C6 ($p < 0.05$, Fig. 5). The FBN-C AUC of w/o and Tofacitinib [100 μ m] were also lower than TGF- β [80 pM] ($p < 0.01$, Fig. 5H).

TGF- β +Tofacitinib [100 μ m] did not statistically reduce the effect of TGF- β on PRO-C1 on any days or PRO-C1 AUC (Fig. 5A-B). However, the PRO-C1 AUC of the control and Tofacitinib [100 μ m] were 95% lower than the TGF- β AUC (Fig. 5B). TGF- β +Tofacitinib [100 μ m] reduced the PRO-C1 AUC response by 48% compared to TGF- β , and the lower doses of Tofacitinib reduced the PRO-C1 AUC response by 15% compared to TGF- β (Fig. 5B). TGF- β +Tofacitinib [100 μ m] and [50 μ m] reduced the PRO-C3 response on day 12 compared to TGF- β ($p < 0.05$, Fig. 5C). There was no statistical significance between any of the PRO-C3 AUCs; however, both the control and Tofacitinib [100 μ m] had a PRO-C3 AUC 94% lower than TGF- β (Fig. 5D). Additionally, did the Tofacitinib doses (100 μ m, 50 μ m, 25 μ m, and 12.5 μ m, respectively) inhibit PRO-C3 AUC response by 78%, 71%, 59%, and 51% compared to TGF- β (Fig. 5D). The PRO-C6 response of TGF- β was not inhibited by any dose of Tofacitinib (Fig. 5E-F). The PRO-C6 AUC of the control and Tofacitinib [100 μ m] were 75% and 84% lower than TGF- β alone (Fig. 5F). TGF- β +Tofacitinib [100 μ m]

reduced the PRO-C6 AUC by 57% compared to TGF- β , while the lower doses of tofacitinib were in the range of the TGF- β response $\pm 10\%$ (Fig. 5F). The FBN-C response was only affected by TGF- β +Tofacitinib [12.5 μ m] on day 12 (Fig. 5G). The FBN-C AUC of the control and Tofacitinib [100 μ m] was lower than TGF- β ($p < 0.01$, Fig. 5H). Neither of the Tofacitinib doses significantly reduced the FBN-C AUC of TGF- β ; however, Tofacitinib [100 μ m] reduced the AUC by 28% (Fig. 5H). The lower doses of tofacitinib increased the FBN-C AUC by 12–26% compared to TGF- β (Fig. 5H).

Discussion

In this study, we investigated the formation of ECM proteins from primary joint FLS in an in vitro model using macromolecular crowders called the Scar-in-a-Jar (Sia) model. We characterized the FLS's response to fibrotic growth factors in the model by measuring the protein levels with biomarkers in 13 FLS donors. The growth factors increased the protein levels, and the inhibitors of fibrosis decreased the protein levels. Our findings demonstrate that the growth factor, TGF- β , promotes increased fibronectin turnover and formation of type I, III, and VI collagens in FLS. We observed that ALK5i and nintedanib could inhibit the fibrotic response induced by TGF- β stimulation in all assessed ECM biomarkers.

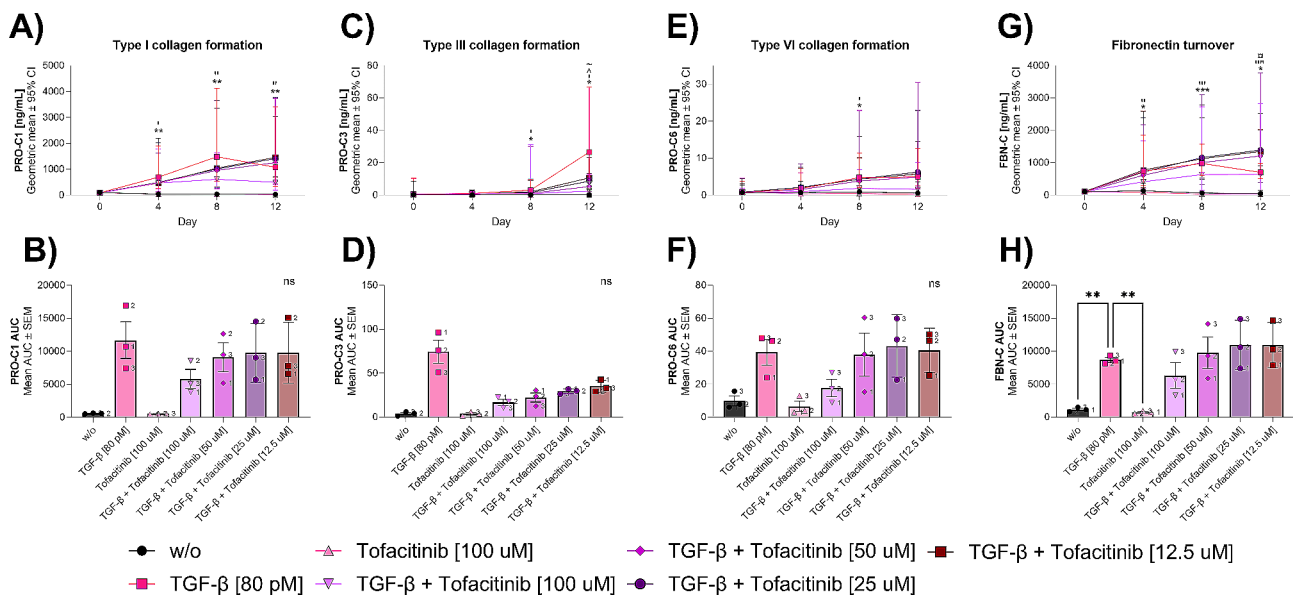


Fig. 5 The inhibitory effect of tofacitinib on TGF- β induction. The data are shown as the geometric mean \pm 95% CI of each biomarker over the 12 days: type I (A), type III (C), type VI (E) collagen formation, and fibronectin turnover (G). The AUC is shown as mean AUC \pm SEM: type I (B), type III (D), type VI (F) collagen formation, and fibronectin turnover (H). Each symbol represents a patient; three donors were used: donors 1, 2, and 3. The symbols and numbers indicate the different donors. The biomarker values were log-transformed to obtain a normal distribution and were compared with two-way ANOVA with Dunnett's multiple comparisons test on different days. The AUC was computed based on the raw biomarker values and then compared with one-way repeated measures ANOVA with Dunnett's multiple comparisons tests. P -values ≤ 0.05 were considered statistically significant. Asterisks indicate: * $p < 0.05$, ** $p < 0.01$, *** $p < 0.001$, and **** $p < 0.0001$. In the time overview, different symbols indicate the comparisons to TGF- β : \bullet w/o, \triangle Tofacitinib [100 μ m], \blacktriangle TGF- β + Tofacitinib [100 μ m], \diamond TGF- β + Tofacitinib [50 μ m], and \square TGF- β + Tofacitinib [12.5 μ m]

Additionally, tofacitinib indicated a tendency to inhibit the fibrotic response in the assessed biomarkers.

Studies in the literature have identified the presence of various types of collagens and fibronectin in the OA and RA synovium and upregulation of collagen gene expression [6, 7, 10–15, 17, 18]. However, the reflection of gene expression on protein levels and fibrogenesis is unknown [19]. In our study, the non-stimulated FLS in the SiaJ model did not produce any of the assessed ECM proteins. This indicates the SiaJ model does not provoke a fibrotic response in the 13 FLS donors tested. Furthermore, the FLS had no inherent predisposition for excessive fibrotic response. When the FLS were stimulated with TGF- β , there was an increase in fibronectin turnover, type I, and VI collagen formation from day 4, with a subsequent increase in type III collagen formation from day 8. The differential induction times may suggest that FLS initially deposits fibronectin, type I, and VI collagen, followed by a secondary deposition of type III collagen. This could be due to a requirement of continuous TGF- β stimulation for initiating type III collagen formation or the potential involvement of other ECM components in triggering the production of type III collagen. However, the pattern with subsequent deposition of type III collagen to fibronectin, type I, and VI collagen formation is also observed in dermal and pulmonary fibroblasts after TGF- β stimulation in the SiaJ model [27–29]. Thus, it might be a general response to TGF- β stimulation in FLS and fibroblasts. The increase in fibrogenesis biomarkers in our study correlates with the upregulation of type I and III collagen gene expression and the presence of fibronectin observed in patients with RA [12, 14, 15]. Similar observations have been detected in OA joints, where TGF- β induces type I collagen, fibronectin, and fibrosis (indicated by staining of collagen fibers) [6, 12, 17, 42]. Thus, TGF- β stimulation of primary FLS imitates an expression profile similar to RA and OA joints.

Our study demonstrates that TGF- β can induce a fibrotic response consistently in multiple joint FLS donors. Inhibiting the fibrotic response triggered by TGF- β is relevant, as there is a substantial amount of TGF- β in the articular cartilage and joint fluid of both patients with RA and OA [32, 43]. As TGF- β 1 activates TGF β R1/ALK5, inhibition of this receptor is likely to counteract a fibrotic response [32]. ALK5i has been shown to inhibit the upregulated gene expression of type I collagen induced by TGF- β in OA-FLS [30]. However, the effect on protein levels has not been elucidated. In our study, ALK5i inhibited the TGF- β induced increase in protein levels across five FLS donors. Both ALK5i [1000 nM] and ALK5i [100 nM] were able to reduce the TGF- β induced formation of type I, III, and VI collagen. The TGF- β induced fibronectin turnover was only inhibited by ALK5i [1000 nM]. The inhibitory effect of ALK5i

on type I collagen protein formation correlates with the inhibition of gene expression in the literature [30]. The effect of ALK5i on the protein levels in FLS correlates with previous findings in pulmonary fibroblasts, where ALK5i inhibited the same biomarkers [28]. The ALK5i [100 nM] dose inhibited the TGF- β induced fibrotic response to different extents within the four biomarkers. The difference suggests that the different proteins may be induced or inhibited through different pathways in the FLS. The ALK5i [1000 nM] dose caused complete inhibition of the TGF- β response, but this might cause problems in the joint, as TGF- β regulates multiple cellular processes [3].

The effect of nintedanib on joint fibrogenesis has yet to be investigated. Nintedanib, an anti-fibrotic drug used to treat idiopathic pulmonary fibrosis (IPF) and systemic sclerosis (SSc)-associated interstitial lung disease (ILD), has been suggested as a possible treatment for RA-ILD [44]. However, the approval for use in IPF and SSc-ILD was not based on nintedanib's effect on fibrosis but on the drug's ability to reduce the expected decline forced vital capacity (FVC) in patients [45, 46]. Our study shows that nintedanib can halt the fibrotic response of TGF- β reflected by type I, III, and VI collagen protein formation and fibronectin turnover. Our findings correlate with nintedanib's inhibitory effect on type I collagen and fibronectin gene expression and protein levels of type I, III, and VI collagen and fibronectin observed in pulmonary fibroblasts [28, 31]. Nintedanib can reduce the fibrotic response in both pulmonary fibroblasts and joint FLS. Thus, the inhibitory effect on pulmonary fibrosis might also be able to inhibit synovial fibrosis in patients with RA or OA. Additionally, if patients with RA have developed synovial fibrosis alongside pulmonary fibrosis, nintedanib may be effective in treating both conditions.

Tofacitinib is a JAK inhibitor approved as an anti-inflammatory treatment for RA [1]. Besides the anti-inflammatory effect, JAK inhibitors might also have an anti-fibrotic effect. An anti-fibrotic effect has been observed in both SSc-ILD and RA-ILD [41, 47, 48]. In our study, we found a trend of tofacitinib inhibiting the fibrotic response of TGF- β : Tofacitinib [100 μ m] reduced the fibrotic response by 48%, 78%, 43%, and 28% of type I, III, VI collagen formation and fibronectin turnover respectively. The effect of tofacitinib on protein levels has not been investigated in FLS before. However, the inhibitory trend of tofacitinib in our study correlates with Ruscitti et al., who demonstrated that tofacitinib inhibits type I collagen gene expression in RA-FLS induced by co-stimulation of TGF- β and interleukin-6 [33]. Additionally, Lescoat et al. showed that another JAK inhibitor, ruxolitinib, inhibits the gene expression of TGF- β and fibrotic components such as fibronectin and type I and III collagens in mice [49]. The results indicate that

tofacitinib has an inhibitory effect on the protein levels of fibrogenesis, which is in correlation with the effect on gene expression from the literature [33, 49]. Additionally, tofacitinib has also been shown to reduce type I collagen gene expression in the skin and lungs of mice with bleomycin-induced fibrosis [41]. Overall, this indicates that tofacitinib has an anti-fibrotic effect in multiple organs. Our study only investigated the effect in three FLS donors; thus, more investigations are needed to determine the effect of tofacitinib in joint FLS. However, tofacitinib has a potential anti-fibrotic effect on both joint and pulmonary fibroblasts, indicating a potential efficacy across multiple organs associated with RA and its comorbidities.

This study has several limitations; one was the limited availability of primary synovial fibroblasts, which were only available from patients with OA and not RA. However, the 13 FLS donors in our study had a fibrotic response to TGF- β stimulation in the SiaJ model. The FLS were isolated from synovial membranes as they became available. The donors were not included or excluded based on sex or age, and these factors were not considered during our investigations. Both sex and age might affect the synovial membrane; thus, further investigations should potentially take this into account. The diverse responses of the different FLS donors to TGF- β induction and fibrotic inhibitors were both a limitation and a strength of this study, as it indicates how differently patients' cells can respond to the same treatments. We speculate whether there is an association between the high fibrotic response to TGF- β in vitro and the postoperative stiffness and pain that some patients experience. Thus, this should be investigated further in a study where more patient information should be collected. Fibrogenesis in the joints might also be induced by other growth factors that TGF- β ; thus, further investigations should be conducted to determine this. As the inhibition of the response might differ between different target receptors, further investigations should be conducted to determine the effect of other potential anti-fibrotic drugs. Additionally, as synovial fibrosis and synovitis might coexist in the joint, further investigations of the fibrotic response of inflamed and fibro-inflamed joints should be conducted.

Conclusion

We have established an in vitro model for assessing fibrogenesis in primary FLS from joints. The increased fibrotic response was characterized by increased ECM protein levels of fibronectin and type I, III, and VI collagen. We found TGF- β to induce the fibrotic response, which can be halted by both direct and indirect inhibition with the anti-fibrotic substances ALK5i and nintedanib. We also found that the anti-inflammatory drug tofacitinib also halted the fibrotic response to some extent; thus, it may

exert an anti-fibrotic effect. TGF- β stimulation induces fibrogenesis across multiple FLS donors, thus implying that TGF- β increases synovial fibrosis. Anti-inflammatory and anti-fibrotic drugs can reduce the TGF- β induced fibrogenesis in vitro. Thus, the drugs might affect patients with rheumatic diseases similarly.

Abbreviations

| | |
|---------------|---|
| ALK | Activin Receptor-like Kinase |
| ANOVA | Analysis of Variance |
| AUC | Area Under the Curve |
| BMP | Bone Morphogenic Protein |
| CI | Confidence Interval |
| DMEM | Dulbecco's Modified Eagle Medium |
| ECM | Extracellular matrix |
| ELISAs | Enzyme-Linked Immunosorbent Assays |
| FBN-C | Biomarker for fibronectin turnover |
| FBS | Fetal Bovine Serum |
| FLS | Fibroblast-like Synoviocytes |
| FVC | Forced Vital Capacity |
| ILD | Interstitial Lung Disease |
| IPF | Idiopathic Pulmonary Fibrosis |
| JAK | Janus kinase (inhibitor) |
| OA | Osteoarthritis |
| P/S | Penicillin/Streptomycin |
| PBS | Phosphate-Buffered Saline |
| PRO-C1 | Biomarker of type I collagen formation |
| PRO-C3 | Biomarker of type III collagen formation |
| PRO-C6 | Biomarker of type VI collagen formation |
| RA | Rheumatoid Arthritis |
| RA-ILD | Rheumatoid arthritis-associated Interstitial Lung Disease |
| RPMI | Roswell Park Memorial Institute (medium) |
| SiaJ | Scar-in-a-Jar |
| SMAD | Suppressor of Mothers Against Decapentaplegic |
| SSc | Systemic Sclerosis |
| SSc-ILD | Systemic Sclerosis-associated Interstitial Lung Disease |
| TGF- β | Transforming growth factor-beta |
| TGF β R | Transforming growth factor-beta receptor |
| w/o | Without (non-stimulated) |

Supplementary Information

The online version contains supplementary material available at <https://doi.org/10.1186/s41231-024-00180-0>.

Supplementary Material 1

Acknowledgements

We want to thank all the patients who volunteered to participate in this study by donating their synovial membranes and cartilage to research after a total knee replacement surgery at Gentofte Hospital, Denmark. We want to thank the doctors, nurses, and staff members at the Orthopedic Surgery Unit, Gentofte Hospital, for conducting the surgeries and preparing the synovial membranes. We want to thank Research Technician Helene S. Hector for initiating the isolation of FLS and helping with experiments. Additionally, we would like to thank Senior Statistician Peder Frederiksen for guiding and engaging in the statistical discussions.

Author contributions

SFM and CST formulated the research goals. SFM performed experiments, analyzed and visualized the data, oversaw the project, wrote the original draft, and edited the final version. SSM performed experiments. ASM and MRA provided the synovial membranes. ACBJ and CST provided resources and supervision. SSM, ASM, MRA, ACBJ, and CST critically reviewed and edited the manuscript. All authors have read and approved the final version of the manuscript.

Funding

SFM has received a PhD grant from The Danish Research Foundation. Open access funding provided by Copenhagen University

Data availability

The data generated during the current study are available from the corresponding author on reasonable request.

Declarations

Ethics approval and consent to participate

The study was conducted in accordance with the Declaration of Helsinki, and all patients gave written informed consent prior to surgery. The collection was approved by the Danish Scientific Ethical Commission (protocol no. H-D-2007-0084).

Consent for publication

All patients gave written informed consent prior to surgery, including consent for publication.

Competing interests

ACBJ and CST are employed and own stocks in Nordic Bioscience A/S. SSM is employed at Eli Lilly Denmark A/S. SFM, ASM, and MRA have nothing to disclose.

Received: 23 February 2024 / Accepted: 23 May 2024

Published online: 01 June 2024

References

- Smolen JS, Aletaha D, Barton A, Burmester GR, Emery P, Firestein GS, et al. Rheumatoid arthritis. *Nat Rev Dis Prim*. 2018;4:18001.
- Martel-Pelletier J, Barr AJ, Cicuttini FM, Conaghan PG, Cooper C, Goldring MB, et al. Osteoarthritis. *Nat Rev Dis Prim*. 2016;2:16072.
- Remst DFG, Blaney Davidson EN, van der Kraan PM. Unravelling osteoarthritis-related synovial fibrosis: a step closer to solving joint stiffness. *Rheumatology (Oxford)*. 2015;54(11):1954–63.
- Chu CQ, Field M, Abney E, Zheng RQ, Allard S, Feldmann M, et al. Transforming growth factor-beta 1 in rheumatoid synovial membrane and cartilage/pannus junction. *Clin Exp Immunol*. 1991;86(3):380–6.
- Lettesjö H, Nordström E, Ström H, Nilsson B, Glinghammar B, Dahlstedt L, et al. Synovial fluid cytokines in patients with rheumatoid arthritis or other arthritic lesions. *Scand J Immunol*. 1998;48(3):286–92.
- Oehler S, Neureiter D, Meyer-Scholten C, Aigner T. Subtyping of osteoarthritic synoviopathy. *Clin Exp Rheumatol*. 2002;20(5):633–40.
- Haraoui B, Pelletier JP, Cloutier JM, Faure MP, Martel-Pelletier J. Synovial membrane histology and immunopathology in rheumatoid arthritis and osteoarthritis. In vivo effects of antirheumatic drugs. *Arthritis Rheum*. 1991;34(2):153–63.
- Sergeant JC, Hyrich KL, Anderson J, Kopec-Harding K, Hope HF, Symmons DPM, et al. Prediction of primary non-response to methotrexate therapy using demographic, clinical and psychosocial variables: results from the UK Rheumatoid Arthritis Medication Study (RAMS). *Arthritis Res Ther*. 2018;20:147.
- Duong SQ, Crowson CS, Athreya A, Atkinson EJ, Davis JM, Warrington KJ, et al. Clinical predictors of response to methotrexate in patients with rheumatoid arthritis: a machine learning approach using clinical trial data. *Arthritis Res Ther*. 2022;24:162.
- Smith MD. The normal synovium. *Open Rheumatol J*. 2011;5:100–6.
- Levick JR, McDonald JN. Microfibrillar meshwork of the synovial lining and associated broad banded collagen: a clue to identity. *Ann Rheum Dis*. 1990;49:31–6.
- Scott DL, Wainwright AC, Walton KW, Williamson N. Significance of fibronectin in rheumatoid arthritis and osteoarthritis. *Ann Rheum Dis*. 1981;40:142–53.
- Eyre DR, Muir H. Type III collagen: a major constituent of rheumatoid and normal human synovial membrane. *Connect Tissue Res*. 1975;4(1):11–6.
- Micheroli R, Elhai M, Edalat S, Frank-Bertoncelj M, Bürki K, Ciurea A et al. Role of synovial fibroblast subsets across synovial pathotypes in rheumatoid arthritis: a deconvolution analysis. *RMD open*. 2022;8:e001949.
- Dennis GJ, Holweg CTJ, Kummerfeld SK, Choy DF, Setiadi AF, Hackney JA, et al. Synovial phenotypes in rheumatoid arthritis correlate with response to biologic therapeutics. *Arthritis Res Ther*. 2014;16:R90.
- Nanus DE, Badoume A, Wijesinghe SN, Halsey AM, Hurley P, Ahmed Z, et al. Synovial tissue from sites of joint pain in knee osteoarthritis patients exhibits a differential phenotype with distinct fibroblast subsets. *EBioMedicine*. 2021;72:103618.
- Remst DFG, Blaney Davidson EN, Vitters EL, Blom AB, Stoop R, Snabel JM, et al. Osteoarthritis-related fibrosis is associated with both elevated pyridinoline cross-link formation and lysyl hydroxylase 2b expression. *Osteoarthr Cartil*. 2013;21(1):157–64.
- Vaamonde-Garcia C, Malaise O, Charlier E, Deroyer C, Neuville S, Gillet P, et al. 15-Deoxy- Δ -12, 14-prostaglandin J2 acts cooperatively with prednisolone to reduce TGF- β -induced pro-fibrotic pathways in human osteoarthritic fibroblasts. *Biochem Pharmacol*. 2019;165:66–78.
- Remst DFG, Blom AB, Vitters EL, Bank RA, van den Berg WB, Blaney Davidson EN, et al. Gene expression analysis of murine and human osteoarthritis synovium reveals elevation of transforming growth factor β -responsive genes in osteoarthritis-related fibrosis. *Arthritis Rheumatol*. 2014;66(3):647–56.
- Kjelgaard-Petersen C, Siebuhr AS, Christiansen T, Ladel C, Karsdal M, Bay-Jensen A-C. Synovitis biomarkers: ex vivo characterization of three biomarkers for identification of inflammatory osteoarthritis. *Biomarkers*. 2015;20(8):547–56.
- Benny P, Raghunath M. Making microenvironments: a look into incorporating macromolecular crowding into in vitro experiments, to generate biomimetic microenvironments which are capable of directing cell function for tissue engineering applications. *J Tissue Eng*. 2017;8:2041731417730467.
- Chen CZC, Peng YX, Wang ZB, Fish PV, Kaar JL, Koepsel RR, et al. The scar-in-a-Jar: studying potential antifibrotic compounds from the epigenetic to extracellular level in a single well. *Br J Pharmacol*. 2009;158(5):1196–209.
- Puerta Cavanzo N, Bigaeva E, Boerema M, Olinga P, Bank RA. Macromolecular crowding as a tool to screen anti-fibrotic drugs: the scar-in-a-Jar system revisited. *Front Med*. 2020;7:615774.
- Chen CZ, Raghunath M. Focus on collagen: in vitro systems to study fibrogenesis and antifibrosis state of the art. *Fibrogenesis Tissue Repair*. 2009;2:7.
- Lareu RR, Subramhanya KH, Peng Y, Benny P, Chen C, Wang Z, et al. Collagen matrix deposition is dramatically enhanced in vitro when crowded with charged macromolecules: the biological relevance of the excluded volume effect. *FEBS Lett*. 2007;581(14):2709–14.
- Good RB, Eley JD, Gower E, Butt G, Blanchard AD, Fisher AJ, et al. A high content, phenotypic 'scar-in-a-jar' assay for rapid quantification of collagen fibrillogenesis using disease-derived pulmonary fibroblasts. *BMC Biomed Eng*. 2019;1:14.
- Madsen SF, Sand JMB, Juhl P, Karsdal M, Thudium CS, Siebuhr AS, et al. Fibroblasts are not just fibroblasts: clear differences between dermal and pulmonary fibroblasts' response to fibrotic growth factors. *Sci Rep*. 2023;13:9411.
- Rønnow SR, Dabbagh RQ, Genovese F, Nanthakumar CB, Barrett VJ, Good RB, et al. Prolonged scar-in-a-jar: an in vitro screening tool for anti-fibrotic therapies using biomarkers of extracellular matrix synthesis. *Respir Res*. 2020;21:108.
- Juhl P, Bondesen S, Hawkins CL, Karsdal MA, Bay-Jensen A-CC, Davies MJ, et al. Dermal fibroblasts have different extracellular matrix profiles induced by TGF- β , PDGF and IL-6 in a model for skin fibrosis. *Sci Rep*. 2020;10:17300.
- Remst DFG, Blaney Davidson EN, Vitters EL, Bank RA, van den Berg WB, van der Kraan PM. TGF- β induces Lysyl hydroxylase 2b in human synovial osteoarthritic fibroblasts through ALK5 signaling. *Cell Tissue Res*. 2014;355:163–71.
- Rangarajan S, Kurundkar A, Kurundkar D, Bernard K, Sanders YY, Ding Q, et al. Novel mechanisms for the antifibrotic action of nintedanib. *Am J Respir Cell Mol Biol*. 2016;54(1):51–9.
- van der Kraan PM. Differential Role of transforming growth factor-beta in an osteoarthritic or a healthy joint. *J bone Metab*. 2018;25(2):65–72.
- Ruscitti P, Liakouli V, Panzera N, Angelucci A, Berardicurti O, Di Nino E et al. Tofacitinib may inhibit myofibroblast differentiation from rheumatoid-fibroblast-like synoviocytes induced by TGF- β and IL-6. *Pharmaceuticals (Basel)*. 2022;15(5).
- Siebuhr AS, Karsdal M, Juhl P, Bay-Jensen AC. Tofacitinib and nintedanib modulate collagen formation in dermal fibroblasts. *Ann Rheum Dis*. 2020;79:1383–1384.
- Yang W, Pan L, Cheng Y, Wu X, Tang B, Zhu H et al. Nintedanib alleviates pulmonary fibrosis in vitro and in vivo by inhibiting the FAK/ERK/S100A4 signalling pathway. *Int Immunopharmacol*. 2022;113:109409.

36. Hostettler KE, Zhong J, Papakonstantinou E, Karakiulakis G, Tamm M, Seidel P et al. Anti-fibrotic effects of nintedanib in lung fibroblasts derived from patients with idiopathic pulmonary fibrosis. *Respir Res.* 2014;15:157.
37. Leeming DJ, Larsen DV, Zhang C, Hi Y, Veidal SS, Nielsen RH, et al. Enzyme-linked immunosorbent serum assays (ELISAs) for rat and human N-terminal pro-peptide of collagen type I (PINP)--assessment of corresponding epitopes. *Clin Biochem.* 2010;43(15):1249–56.
38. Nielsen MJ, Nedergaard AF, Sun S, Veidal SS, Larsen L, Zheng Q, et al. The neo-epitope specific PRO-C3 ELISA measures true formation of type III collagen associated with liver and muscle parameters. *Am J Transl Res.* 2013;5(3):303–15.
39. Sun S, Henriksen K, Karsdal MA, Byrjalsen I, Rittweger J, Armbrecht G, et al. Collagen type III and VI turnover in response to long-term immobilization. *PLoS ONE.* 2015;10(12):1–14.
40. Bager CL, Gudmann N, Willumsen N, Leeming DJ, Karsdal MA, Bay-Jensen AC, et al. Quantification of fibronectin as a method to assess ex vivo extracellular matrix remodeling. *Biochem Biophys Res Commun.* 2016;478(2):586–91.
41. Wang W, Bhattacharyya S, Marangoni RG, Carns M, Dennis-Aren K, Yeldandi A, et al. The JAK/STAT pathway is activated in systemic sclerosis and is effectively targeted by tofacitinib. *J Scleroderma Relat Disord.* 2020;5(1):40–50.
42. Wei Q, Kong N, Liu X, Tian R, Jiao M, Li Y, et al. Pirfenidone attenuates synovial fibrosis and postpones the progression of osteoarthritis by anti-fibrotic and anti-inflammatory properties in vivo and in vitro. *J Transl Med.* 2021;19:157.
43. Fava R, Olsen N, Keski-Oja J, Moses H, Pincus T. Active and latent forms of transforming growth factor beta activity in synovial effusions. *J Exp Med.* 1989;169(1):291–6.
44. Matteson EL, Kelly C, Distler JHW, Hoffmann-Vold A-M, Seibold JR, Mittoo S, et al. Nintedanib in patients with Autoimmune Disease-Related Progressive Fibrosing interstitial lung diseases: Subgroup Analysis of the INBUILD Trial. *Arthritis Rheumatol.* 2022;74(6):1039–47.
45. Richeldi L, du Bois RM, Raghu G, Azuma A, Brown KK, Costabel U, et al. Efficacy and safety of nintedanib in idiopathic pulmonary fibrosis. *N Engl J Med.* 2014;370(22):2071–82.
46. Distler O, Highland KB, Gahlemann M, Azuma A, Fischer A, Mayes MD, et al. Nintedanib for systemic sclerosis-Associated interstitial lung disease. *N Engl J Med.* 2019;380(26):2518–28.
47. Fiorentini E, Bonomi F, Peretti S, Orlandi M, Lepri G, Matucci Cerinic M et al. Potential role of JAK inhibitors in the treatment of systemic sclerosis-associated interstitial lung disease: a narrative review from pathogenesis to real-life data. *Life (Basel).* 2022;12(12):2101.
48. d'Alessandro M, Perillo F, Metella Refini R, Bergantini L, Bellisai F, Selvi E, et al. Efficacy of baricitinib in treating rheumatoid arthritis: modulatory effects on fibrotic and inflammatory biomarkers in a real-life setting. *Int Immunopharmacol.* 2020;86:106748.
49. Lescoat A, Lelong M, Jeljeli M, Piquet-Pellorce C, Morzadec C, Ballerie A, et al. Combined anti-fibrotic and anti-inflammatory properties of JAK-inhibitors on macrophages in vitro and in vivo: perspectives for scleroderma-associated interstitial lung disease. *Biochem Pharmacol.* 2020;178:114103.

Publisher's Note

Springer Nature remains neutral with regard to jurisdictional claims in published maps and institutional affiliations.